Hindawi
International Journal of Aerospace Engineering
Volume 2019, Article ID 5079738, 16 pages
https://doi.org/10.1155/2019/5079738

Research Article

AOCS Requirements and Practical Limitations for High-Speed Communications on Small Satellites

Fernando Aguado-Agelet,[1,2] **Andrés Eduardo Villa**,[1,2] **Marcos Arias-Acuña**,[1] **and Francisco Javier Díaz-Otero**[1]

[1]*Departamento Teoría de la Señal y Comunicaciones, Universidade de Vigo, 36310, Spain*
[2]*Department of Space, CINAE, Nigrán 36350, Spain*

Correspondence should be addressed to Fernando Aguado-Agelet; faguado@tsc.uvigo.es

Received 13 February 2018; Accepted 12 November 2018; Published 17 February 2019

Academic Editor: Jeremy Straub

In recent years, an increasing number of countries have shown a growing interest in developing their indigenous space capacity building through national small satellite programs. These satellites, which were initially focused on educational and training missions, currently are more scientific and operational-oriented. Thus, small satellite missions are being considered not only as educational tools but also as technological demonstrators or, even, mature enough for commercial and scientific missions, which might generate a huge amount of data to be transmitted to the ground segment. Therefore, an increasing demand on channel capacity will be needed for downloading the generated housekeeping and scientific data for missions based on small satellites. This paper analyses the communication subsystem of a real Cubesat. The influence of geometrical parameters is rigorously calculated both in the signal-to-noise ratio and in the capacity to transmit information. Subsequently, which parameters of the radio link can be modified to increase the transmission capacity, including the pointing requirements and its practical implementation, is studied. Finally, and as a future line, the technical feasibility of using optical links on small satellites that might greatly increase the transmission capacity, including the satellite pointing problems that presents, is presented. In conclusion, this paper presents a rigorous calculation in different frequency bands of the signal-to-noise ratio and the pointing accuracy that is needed to achieve the maximum transmission speed from the satellite to the ground station, and therefore the requirements that the Attitude and Orbital Control Systems (AOCS) must have, as well as the limitations of current systems.

1. Introduction

A small satellite is a spacecraft able to provide, within a low-cost framework, not only educational purposes but also space services and applications, reducing cost, facilitating the launch process as piggybacks or low-weight payloads, using cheaper designs (easing the Assembly, Integration and Verification process), and allowing mission disaggregation.

They are built in quick timescales, at relatively low cost, and make maximum use of state-of-the-art commercial-of-the-shelf (COTS) technologies to achieve complex functionality, while at the same time minimizing dependence on complex mechanisms and deployable structures.

Both the technology evolution and electronics miniaturisation have promoted a fast-growing path for the integration of this sort of spacecrafts in daily applications as well as in the university environment, where the design and development of small satellites provides a highly valuable experience to students and researchers opening up a low-cost space gateway.

The expertise acquired during recent years researching in small satellite communications has led some initiatives [1, 2] into the philosophy of defining the "small satellites" as lean spacecrafts capable of providing, from a low-cost framework, space services and applications, using design, development, and Assembly, Integration and Verification campaigns according to a low-profile application of bigger mission standards.

The Cubesat standard [3] was developed by the California Polytechnic State University (CalPoly) and the Space Systems

Development Laboratory of Stanford University. Its main purpose is to approach space research opportunities to universities by defining a standard mechanical interface and deployment system for small satellites. The basic structure of a Cubesat (1U) is a 10 cm wide cube with a mass of up to 1.3 kg, which is designed to work autonomously. It is a solid and skeleton-like structure made of aluminium whose weight can be reduced. The concept of double, triple, six, and twelve times Cubesats (2U, 3U, 6U, and 12U), with dimensions of $10 \times 10 \times 20$ cm, $10 \times 10 \times 30$ cm, $10 \times 20 \times 30$ cm, and $20 \times 20 \times 30$ cm, respectively (these size increments also entail different increases in the mass of the device), has also been developed.

Cubesats have undergone a large evolution in a few years. From the first Cubesats launched in 2003 - which were mostly test beds for technologies that could be applied to space systems and which were based on COTS components - to current Cubesat missions to provide direct services and applications, there is a really large leap in the development of their technology. The first Cubesats built were mere student projects to provide some experience in space systems. These systems were mostly based on commercial components and had payloads which were purposefully built. Even though these satellites were complete and functional systems, they were not mature enough to sustain a complex mission or guarantee any performance. Lately, Cubesats have been and will be used for missions planned for the future for mainly three kinds of missions:

(i) Technology demonstrators

(ii) Scientific missions

(iii) Services

Currently, the new space industry strongly believes that Cubesats will be used for low-cost space services and missions. One of the main issues regarding the range of missions that Cubesats can perform is the payload accommodation. Cubesats have strict limitations in terms of mass and volume, which is not the common mindset in classical spacecraft design. A payload that carries a couple of Petri boards for a biology experiment may be larger than a Cubesat itself when designed to be integrated, for example, in the International Space Station. Therefore, the challenge is to adapt classical payloads so that they can be integrated in a Cubesat. Two key factors must be taken into account when talking about payload adaptation for Cubesats:

(i) Electronics Miniaturisation. Electronic devices have undergone a miniaturisation trend in the last years. A single chip can provide a whole computer system with very low power consumption, weight, and volume, which makes them ideal for Cubesats.

(ii) Cubesat Cost. Building and launching multiple Cubesats is in most cases much cheaper than building a single payload with an incredible amount or redundancy. This mindset change allows miniaturisation to become a predominant aspect in the design of these spacecrafts.

Currently available orbital deployers are provided by different institutions and/or companies. All these orbital deployers can be employed for injecting Cubesats into appropriate orbits, which will lead to a single satellite or a constellation of satellites that will be able to achieve a certain level of performance.

In Section 2, a complete analysis of the link budget of the Xatcobeo satellite on a UHF radio amateur band is introduced, including how to compute the antenna noise at the spacecraft and the ground station antennas. In Section 3, a number of alternatives to increase the communication capacity are analysed, including the use of higher carrier frequencies, which allows increasing the antenna gain in the satellite and in the ground station, as well as optical links. Finally, a feasibility analysis of AOCS for the different situations is presented.

The readers of this paper, using the rigorous calculation of the signal-to-noise ratio and the pointing accuracy presented in it, can understand the requirements that AOCS must have, as well as the limitations of current systems in different frequency bands.

2. Xatcobeo Satellite

Xatcobeo [4] was the first satellite designed, manufactured, and operated by the University of Vigo. It was launched on the Vega maiden flight, as part of the Educational Payload, and it can be considered as an example of a typical university Cubesat demanding a reduced transmission capacity. It was selected as an educational project focused on providing hands-on experience to undergraduate and PhD students. This Cubesat included two payloads: a software configurable radio and a system for measuring the amount of ionizing radiation. There was also an experimental system for solar panel deployment validation. Xatcobeo was launched on February 13, 2011, and re-entried on August 31, 2014.

This section presents the Xatcobeo [5] communication subsystem, including a complete analysis of the link budget.

2.1. Xatcobeo Communication Subsystem. The housekeeping and scientific data generated in a typical orbit of Xatcobeo was only 1565 bytes. Considering 29 data bytes per frame, only 54 frames were necessary to transmit the complete gathered data in each orbit. Therefore, a 1200 bps communication link was enough for guaranteeing the necessary data exchange. The COTS Telemetry, Tracking and Control subsystem NanoCom U480 developed by GomSpace complied all the communication requirements, and it was successfully used during the mission.

2.2. Xatcobeo Link Budget. The link budget is the comparison among the power given to the transmitter, the amount of power available in the receiver, and the noise at the same point of the receiver.

When a communication satellite is used, there are two different link budgets, the uplink (from the ground station to the satellite) and the downlink (from the satellite to the ground station).

Table 1: Orbital parameters (inputs).

STK input	Value
Orbit epoch	June 1, 2009, 12:00:00.000 UTCG
Start time	June 1, 2009, 12:00:00.000 UTCG
Stop time	February 1, 2010, 12:00:00.000 UTCG
Propagator	High-precision orbit propagator
Step size	60 s
Coordinate type	Classical
Coordinate system	J2000
Apogee altitude	1447 km
Perigee altitude	354 km
Inclination	71°
Argument of perigee	0°
RAAN	0°
True anomaly	90°

Table 2: Orbital parameters (outputs).

STK output	Value
Semimajor axis	7278.64 km
Mean motion	13.9807 revs/day
Eccentricity	0.0750827
Period	6179.97 s

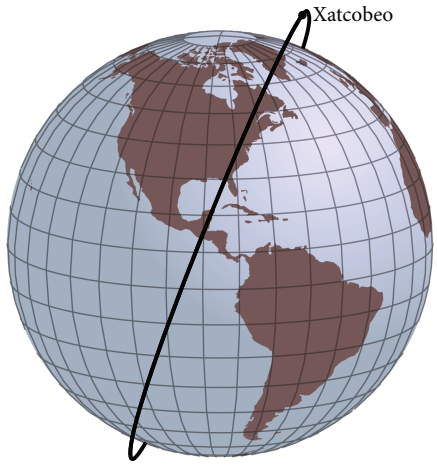

Figure 1: Xatcobeo's orbit.

The first step previous to calculating the link budgets is the determination of the parameters of the orbit of the satellite, which gives us the parameters needed to calculate the link budgets.

2.2.1. General Parameters of the Link Budget Analysis. The orbital analysis of the Xatcobeo mission was performed using the Systems Tool Kit (STK) program [6]. Table 1 shows the parameters used in the analysis.

STK program output values are shown in Table 2 and the orbit in Figure 1.

2.2.2. Rf Environment Parameters. The frequency assigned to Xatcobeo was 437.365 MHz, so the wavelength was 0.6859 m.

The modulation used was FM so the minimum signal-to-noise ratio (SNR) was 12 dB and the bandwidth 6 kHz for a transmission of 1200 bps.

The location of the ground station gives inputs of the STK program (Table 3).

Using the STK program, the mean duration of access was calculated. The satellite gave almost 14 revolutions per day, but only 7 with access with the ground station. Usually, only 3 of these passes were useful, because the satellite did not transmit in eclipse. The amount of data that could be transferred from the satellite to the ground station was calculated in Table 4 as a function of the elevation angle β.

It can be observed in Table 4 that using 5° of elevation allowed transferring a 33% more data than using 15°.

Losses produced by rain, gas, and tropospheric scintillation were calculated for both the uplink and the downlink, applying the models that are explained in the next sections. The Earth temperature considered was 290 K.

2.2.3. Antennas and Polarization Losses. The Xatcobeo satellite did not have a pointing mechanism. The antenna used at the satellite was a turnstile with circular polarization on its axis, but as the satellite was rotating, so did the polarization change among vertical, horizontal, and circular. In the worst case (99% of the time), the gain of this antenna is −6 dBi.

The ground station used a Yagi antenna with a gain of 18.95 dBi and two connectors, for vertical and horizontal polarization. In order to increase the link time, the ground station was designed using a diversity scheme to obtain the signal from ever possible polarization of the incident wave, using the two outputs of the antenna [7]. Then, the worst case produced polarization losses of PLF = 3 dB.

2.2.4. Free Space Losses. Free space losses are given by

$$L_{\mathrm{FS}} = 20 \log \left(\frac{4\pi r}{\lambda}\right), \tag{1}$$

where r is the distance between the transmitter and the receiver, and it must be calculated in the best and worst cases. The best case was the perigee altitude where $H = 354$ km. The worst case happened when the satellite had a minimum elevation β and its altitude H was the apogee one (1447 km), and in this case, the maximum distance is

$$r_{\max} = \sqrt{R_{\mathrm{E}}^2 \sin^2\beta + 2HR_{\mathrm{E}} + H^2} - R_{\mathrm{E}} \sin\beta, \tag{2}$$

and the values are shown in Table 5.

Free space losses for the best case were 136.24 dB, so in the worst case, the difference between maximum and minimum received power was 21.09 dB when the elevation was 5°.

2.2.5. Atmospheric Losses. The atmospheric losses represent the contribution of the rain losses L_{RAIN} [8] and the gaseous absorption losses L_{GAS} [9]. The STK program provides the values in Table 6 of atmospheric losses $L_{\mathrm{ATM}} = L_{\mathrm{RAIN}} + L_{\mathrm{GAS}}$.

Table 3: Ground station parameters.

STK input	Value
Latitude	42.2371°
Longitude	−8.7216°
Altitude	Terrain data files of STK

Table 4: Maximum data transfer per day.

Outputs	$\beta = 5^\circ$	$\beta = 10^\circ$	$\beta = 15^\circ$
Minimum duration of access (min)	0.64	0.24	0.02
Maximum duration of access (min)	20.2	17.62	15.36
Mean duration of access (min)	11.55	10.01	8.68
Mean duration of access per day (min)	34.65	30.03	26.04
Maximum data transmitted per day (Mbit)	2.38	2.06	1.79

Table 5: Maximum distance to the satellite and free space losses.

Outputs	$\beta = 5^\circ$	$\beta = 10^\circ$	$\beta = 15^\circ$
r_{max} (km)	4011	3559	3174
L_{FS} (dB)	157.33	156.29	155.30

Table 6: Atmospheric losses.

Elevation	$\beta = 5^\circ$	$\beta = 10^\circ$	$\beta = 15^\circ$
Maximum L_{ATM} (dB)	0.22	0.11	0.08
Mean L_{ATM} (dB)	0.11	0.07	0.05
Minimum L_{ATM} (dB)	0.02	0.02	0.02

Table 7: Losses by tropospheric scintillation.

Elevation	$\beta = 5^\circ$	$\beta = 10^\circ$	$\beta = 15^\circ$
Maximum L_S (dB)	0.37	0.16	0.10
Mean L_S (dB)	0.16	0.09	0.06
Minimum L_S (dB)	0.02	0.02	0.02

Only maximum losses were considered because this was the worst case.

2.2.6. Tropospheric Scintillation Losses. STK computes the loss in dB that occurs for the percentage time not exceeding the specified limit. To use the tropospheric scintillation model, a tropospheric fade outage of 0.1% was selected.

The other parameter required was the percent time refractivity gradient < −100 N units/km (used 20%). This information was not available electronically and had to be entered manually from the International Telecommunication Union charts.

Table 7 presents the results for different elevation angles.

Table 8: Doppler deviation.

Elevation	$\beta = 5^\circ$	$\beta = 10^\circ$	$\beta = 15^\circ$
Relative velocity (km/s)	7.07	6.99	6.85
Frequency deviation (kHz)	10.3	10.2	10.0

2.2.7. Unpointing Antenna Loss. Losses by unpointing of the antennas L_{up} were considered as 1 dB (typical value).

2.2.8. Doppler Shift. The Doppler shift is defined as the maximum difference in the carrier frequency due to the Doppler effect:

$$\Delta f = \frac{v_{rel}}{c} \cdot f, \quad (3)$$

where Δf is the Doppler shift, v_{rel} is the relative speed of the satellite with respect to the ground station, and f is the central carrier frequency 437.365 MHz.

In order to calculate the Doppler shift, a geometrical study of the orbit must be accomplished, giving as a result that the maximum Doppler shift happens when the satellite has a minimum elevation β, its altitude is the perigee one, and the direction is towards the ground station.

The speed of the Xatcobeo satellite at its perigee was calculated with STK giving 7.49 km/s. This Doppler deviation (Table 8) produced that the filter bandwidth must be increased in 20.6 kHz or the central frequency must be variable in order to take into account the Doppler deviation calculated in terms of the instant position of the satellite.

In Xatcobeo's receiver, the frequency Auto Track option that allows a receiver to track and lock onto the transmitter's carrier frequency with which it is currently linking, including any Doppler shift, was used. This allows using a bandwidth of only 6 kHz.

2.3. Xatcobeo's Downlink. The transmission line is shown in Figure 2.

2.3.1. Received Power. The minimum SNR was calculated at the input of the receiver with sensitivity 0.18 μV = −151.88 dBW. Predemodulation gains and losses were $G_{rx} = -0.45 - 0.9 - 0.09 + 20 - 0.92 = 17.64$ dB.

The signal level at the input of the receiver, using the values from previous sections and Figure 2, was

$$P_r = P_t + G_t - L_{FS} - L_{ATM} - L_S - L_{UP} + PLF + G_r + G_{rx}, \quad (4)$$

and the result is shown in Table 9.

2.3.2. Antenna Temperature. The antenna temperature will be the result of the contribution of galactic noise temperature t_{ext}, ground temperature t_{ground}, sun temperature t_{sun}, and artificial noise temperature t_{art}, all of them weighted by the antenna gain

$$t_a = \frac{1}{4\pi} \oiint \left(t_{ext} + t_{ground} + t_{sun} + t_{art}\right) g(\theta, \phi) \sin\theta d\theta d\phi. \quad (5)$$

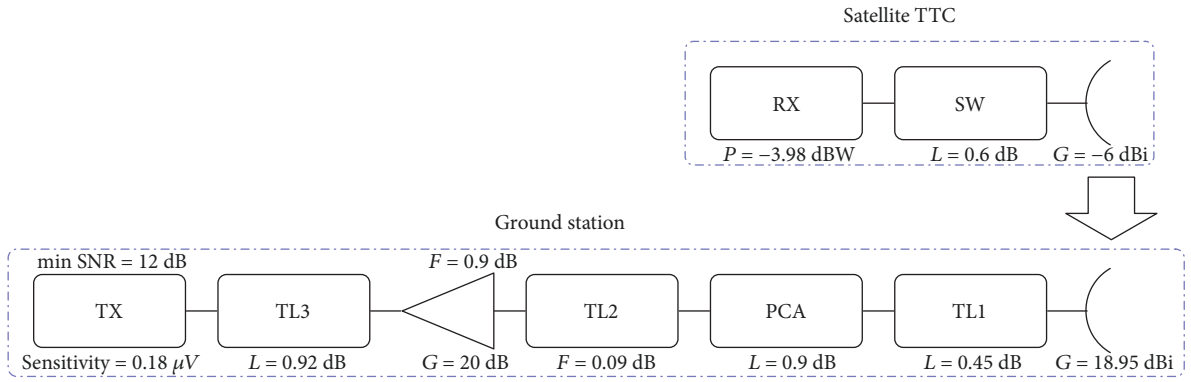

Figure 2: Downlink transmission line.

Table 9: Signal level at the input of the receiver (downlink).

Elevation	$\beta = 5^\circ$	$\beta = 10^\circ$	$\beta = 15^\circ$
P_t (dBW)	−4.58	−4.58	−4.58
G_t (dBi)	−6.00	−6.00	−6.00
L_{FS} (dB)	157.33	156.29	155.30
L_{ATM} (dB)	0.22	0.11	0.08
L_S (dB)	0.37	0.16	0.10
L_{up} (dB)	1.00	1.00	1.00
PLF (dB)	−3.00	−3.00	−3.00
G_r (dBi)	18.95	18.95	18.95
Received power at antenna output (dBW)	−153.55	−152.19	−151.11
G_{rx} (dB)	17.64	17.64	17.64
P_r (dBW)	−135.91	−134.55	−133.47
Margin with sensitivity (dB)	15.97	17.33	18.41

In order to calculate every contribution, the antenna must be modeled by an analytical function [10]

$$g(\theta) = 2(2q+1)\cos^{2q}\theta. \tag{6}$$

As the receiver antenna had a gain of 18.95 dBi = 78.52, $q = 19.13$, and the antenna was modeled as

$$g(\theta) = 78.52\cos^{38.26}\theta, \tag{7}$$

for values $\theta \le \pi/2$.

Artificial noise was neglected due to that the ground station was located at Vigo University Campus, far from the city and industries.

Sun noise was calculated in the worst case, assuming that the antenna was pointing at the sun with a half degree beamwidth (8.73 mrad) and a temperature of 290,000 K at this frequency [11].

Galactic noise (100 K) was considered for all ϕ angles for $\theta < \beta$ and for $\theta \ge \beta$ only for the upper half space ($\phi \ge \pi$). Ground noise (290 K) was considered for the remaining directions

$$\begin{aligned} t_a = \frac{1}{4\pi}\Bigg[&\int_0^{2\pi}\int_0^{\beta} 100\cdot g(\theta,\phi)\sin\theta d\theta d\phi \\ &+ \int_{\pi}^{2\pi}\int_{\beta}^{\pi/2} 100\cdot g(\theta,\phi)\sin\theta d\theta d\phi \\ &+ \int_0^{\pi}\int_{\beta}^{\pi/2} 290\cdot g(\theta,\phi)\sin\theta d\theta d\phi \\ &+ \int_{\pi}^{2\pi}\int_0^{0.00436} 290000\cdot g(\theta,\phi)\sin\theta d\theta d\phi\Bigg]. \end{aligned} \tag{8}$$

Using the expression (7) of the gain into (8), the antenna temperature was

$$\begin{aligned} t_a = 39.26\cdot\Bigg[&\int_0^{\beta}\cos^{38.26}\theta\sin\theta d\theta \\ &+ \frac{100}{2}\cdot\int_{\beta}^{\pi/2}\cos^{38.26}\theta\sin\theta d\theta \\ &+ \frac{290}{2}\cdot\int_{\beta}^{\pi/2}\cos^{38.26}\theta\sin\theta d\theta + 290000 \\ &\cdot\int_0^{0.00436}\cos^{38.26}\theta\sin\theta d\theta\Bigg]. \end{aligned} \tag{9}$$

Solving the integral (9)

$$\begin{aligned} t_a &= 100\cdot\Bigg[1-\cos^{39.26}\beta+\frac{1}{3}\cdot\cos^{39.26}\beta+1.45\cdot\cos^{39.26}\beta \\ &\quad + 2900\cdot\cos^{39.26}0.00436\Bigg] \\ &= 100\cdot\left[1+0.95\cos^{39.26}\beta\right]+108.2. \end{aligned} \tag{10}$$

The last term 108.2 K is the contribution of the sun when the antenna was pointing to it. The final results for different elevation angles are shown in Table 10.

Table 10: Antenna temperature (downlink).

Elevation	$\beta = 5^\circ$	$\beta = 10^\circ$	$\beta = 15^\circ$
With sun (K)	289.99	260.28	232.56
Without sun (K)	181.79	152.08	124.36

Table 11: Downlink noise temperature and power.

Elevation	$\beta = 5^\circ$	$\beta = 10^\circ$	$\beta = 15^\circ$
Noise temperature (K)	29,408	27,682	26,721
Noise power (dBW)	−146.14	−146.40	−146.66

2.3.3. Noise Temperature of the Receiver Chain. The receiver (Figure 2) was composed of a transmission line of 5 m with an attenuation of $L_{TL1} = 0.45$ dB ($a_{TL1} = 1.1092$), a polarization commutation accessory with $L_{PCA} = 0.9$ dB ($a_{PCA} = 1.2303$), another transmission line of 1 m with $L_{TL2} = 0.09$ dB ($a_{TL2} = 1.0209$), a low noise amplifier with $G_{AMP} = 20$ dB ($g_{AMP} = 100$) and noise factor $F_{AMP} = 0.9$ dB ($f_{AMP} = 1.2303$), a third transmission line of 15 m and $L_{TL3} = 0.92$ dB ($a_{TL3} = 1.2359$), and finally a receiver with sensitivity of 0.18 μV.

Table 12: Downlink budget.

Elevation	$\beta = 5^\circ$	$\beta = 10^\circ$	$\beta = 15^\circ$
Received power Pr (dBW)	−135.91	−134.55	−133.47
Noise power (dBW)	−146.14	−146.40	−146.66
SNR (dB)	10.23	11.85	13.19
Margin with 12 dB (dB)	−1.77	−0.15	1.19

The total temperature of the receiver chain t_{rx} at the input of the receiver with a physical temperature t_{phy} including the antenna temperature could be calculated (reordering some terms) as

$$t_{rx} = t_a \cdot g_{tx} + \frac{\left(\left(t_{phy}\left(a_{TL1}a_{PCA}a_{TL2} - 1\right)/a_{TL1}a_{PCA}a_{TL2}\right) + 290\left(f_{AMP} - 1\right)\right)g_{amp} + t_{phy}\left(a_{TL3} - 1\right)}{a_{TL3}} + t_{eq_{rx}}, \tag{11}$$

where $g_{tx} = g_{amp}/a_{TL1}a_{PCA}a_{TL2}a_{TL3}$.

The receiver had a sensitivity of 0.18 μV. With an impedance of 50 Ω, and a SNR = 12 dB, the noise power was $4.09 \cdot 10^{-17}$ W. With a bandwidth of 6 kHz, the equivalent noise at the input of the receiver was $t_{eq_{rx}} = 481.1$ K.

Using $t_{phy} = t_0 = 290$ K and the values of the elements of the receiver chain in (11), the relationship between the input temperature at the receiver and the antenna temperature was

$$t_{rx} = 58.08 \cdot \left(t_a + 216.34\right). \tag{12}$$

The last term (216.34 K) is the equivalent temperature of the receiver chain at the antenna output. The total noise temperature and the noise power are shown in Table 11.

2.3.4. Signal-to-Noise Ratio. Comparing the noise power (Table 11) with the signal power (Table 9), the downlink budget for the worst case can be observed in Table 12.

When the elevation was 5° and all the constraints were in the worst possibility (pointing to the sun, apogee distance to the satellite, its antenna radiating in the worst direction and having 3 dB of polarization error and 1 dB of pointing error), there was no reception. But this possibility was extremely unlikely, and it compromised the reception only for a few seconds.

This approximation is pessimistic, but it is important to design the link in the worst situation to ensure that it is going to work always.

The best link budget appeared when the satellite was above the ground station and without additional losses. The result and its comparison are shown in Table 13.

In the best case, the received power was 33.2 dB greater than in the worst case, and the noise was only 2 dB less. The maximum received power is important in ensuring than the low noise amplifier and the receiver operate within the dynamic margin.

2.4. Xatcobeo's Uplink. The transmission line is shown in Figure 3.

2.4.1. Received Power. The minimum SNR was calculated at the input of the receiver with sensitivity −118 dBm = −148 dBW. Losses introduced by the switch after the antenna were 0.6 dB.

The signal level at the input of the receiver, using the values from previous sections and Figure 3, was

$$P_r = P_t + G_t - L_{FS} - L_{ATM} - L_S - L_{UP} + PLF + G_r - L_{SW}, \tag{13}$$

and the result is shown in Table 14.

2.4.2. Antenna Temperature. The antenna temperature will be the result of the contribution of galactic noise temperature t_{ext}, ground temperature t_{ground}, and sun temperature t_{sun}.

$$t_a = \frac{1}{4\pi}\oiint\left(t_{ext} + t_{ground} + t_{sun}\right)g(\theta,\phi)\,\sin\theta d\theta d\phi. \tag{14}$$

In order to calculate every contribution, the antenna was modeled as isotropic. Galactic noise is 2.7 K, and the Earth temperature is 290 K. Assuming that the satellite was close

Table 13: Worst and best case for SNR in downlink.

Situation	Worst case	Best case	Difference (dB)
P_t (dBW)	−4.58	−4.58	0.00
G_t (dBi)	−6.00	1.56	7.56
L_{FS} (dB)	157.33	136.24	21.09
L_{ATM} (dB)	0.22	0.02	0.20
L_S (dB)	0.37	0.02	0.35
L_{up} (dB)	1.00	0.00	1.00
PLF (dB)	−3.00	0.00	−3.00
G_r (dBi)	18.95	18.95	0.00
G_{rx} (dB)	17.64	17.64	0.00
P_r (dBW)	−135.91	−102.71	33.20
Noise temperature (dBK)	44.68	42.64	−2.04
Noise power (dBW)	−146.14	−148.18	−2.04
SNR (dB)	10.23	45.47	35.24

enough to the Earth, the temperature in half space was 290 K and in the other half was 40 K [11], so the antenna temperature was the mean, 165 K.

Sun noise with the antenna with its maximum gain (1.56 dB) was calculated, assuming that the sun occupies half degree (8.73 mrad) and had a temperature of 290,000 K at this frequency [11]:

$$t_a = \frac{1}{4\pi}\left[\int_0^{2\pi}\int_0^{0.00436} 290000 \cdot 1.43 \sin\theta d\theta d\phi = 1.97\,\mathrm{K}\right]. \quad (15)$$

The final antenna temperature for the uplink was then 166.97 K.

2.4.3. Noise Temperature of the Receiver Chain. The receiver (Figure 3) was composed by a switch with an attenuation of $L_{SW} = 0.6$ dB ($a_{SW} = 1.1482$) and the receiver with sensitivity of −118 dBm = −148 dBW.

The receiver had a SNR = 20 dB, then the noise power was −168 dBW. With a bandwidth of 6 kHz, the equivalent noise at the input of the receiver was $t_{receiver} = 191.41$ K.

The total temperature of the receiver chain at the input of the receiver with a physical temperature t_{phy} including the antenna temperature could be calculated (reordering some terms) as

$$t_{rx} = \frac{t_a + t_{phy}(a_{SW} - 1)}{a_{SW}} + t_{receiver}. \quad (16)$$

Using $t_{phy} = t_0 = 290$ K, the input noise temperature at the receiver was 374.26 K. The total noise temperature and the noise power are shown in Table 15.

2.4.4. Signal-to-Noise Ratio. Comparing the noise power (Table 15) with the signal power (Table 14), the uplink budget for the worst case can be observed in Table 16.

In the uplink, there was more than 12.5 dB of margin in every situation. This difference with the downlink was due to the power emitted by the ground station that is more than 20 dB greater than the power emitted by the satellite.

The best link budget appears when the satellite was over the ground station and without additional losses. The result and its comparison are shown in Table 17.

In the best case, the received power was 33.2 dB greater than in the worst case.

3. Increasing the Data Rate for Cubesats

In recent years, several nano- and microsatellites have been launched to carry out Earth Observation missions that require high-speed data links. These small missions are attractive because of their reduced budgets and development times. The amount of data gathered with these platforms is largely unutilized, due to the limited amount and quality of available communications equipment on the market. Table 18 presents the data transmission capacities of several missions that have been flown in the time period 2013-2016. The maximum data rate achieved by the missions analysed is 100 Mbps for the microsatellite-based missions and 200 Mbps for the commercial nanosatellite-based missions.

3.1. Increasing the Received Power without Pointing the Satellite. With the results obtained in the previous section, the SNR can be improved increasing the following parameters:

(i) The minimum elevation angle

(ii) The gain of the ground segment antenna

(iii) The radiated power in the satellite

Increasing the SNR can be used to change the modulation, choosing one with more bits per symbol, or to increase the bit rate using more bandwidth. If we duplicate the bandwidth, then the bit rate can also be duplicated.

With the results obtained in the previous section, increasing the elevation angle from 5 to 15 degrees reduces the access time, but increases the SNR in 2.94 dB, which allows doubling the bandwidth and the bit rate. So, the global increase will be 50% of the total data rate.

Xatcobeo was a 1U Cubesat. Using a 3U or a 6U Cubesat allows increasing the radiating power in a factor of 2 to 10, and the received power increases in the same factor.

The gain of the ground segment antenna is difficult to increase. We used an antenna of 18.95 dBi that is in the limit to be used in an amateur ground station due to its length (5.74 m) and weight (3.4 kg).

3.2. Pointing the Antenna to Nadir. The antenna used in Xatcobeo has 120° [19] of half power beamwidth. Pointing this antenna to the center of the Earth has some losses in the gain because it is not pointed to the ground station. The worst case is when the satellite is near the horizon, where the angle η between the nadir and the

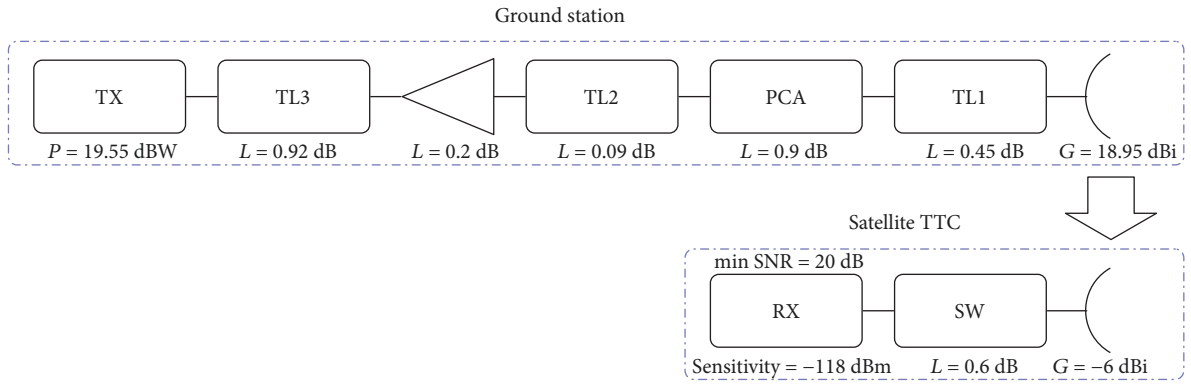

Figure 3: Uplink transmission line.

Table 14: Signal level at the input of the receiver (uplink).

Elevation	$\beta = 5^\circ$	$\beta = 10^\circ$	$\beta = 15^\circ$
P_t (dBW)	16.99	16.99	16.99
G_t (dBi)	18.95	18.95	18.95
L_{FS} (dB)	157.33	156.29	155.30
L_{ATM} (dB)	0.22	0.11	0.08
L_S (dB)	0.37	0.16	0.10
L_{up} (dB)	1.00	1.00	1.00
PLF (dB)	−3.00	−3.00	−3.00
G_r (dBi)	−6.00	−6.00	−6.00
Switch losses L_{SW} (dBi)	0.60	0.60	0.60
Received power P_r (dBW)	−132.58	−131.22	−130.14
Margin with sensitivity (dB)	15.42	16.78	17.86

Table 15: Uplink noise temperature and power.

Parameter	Value
Noise temperature (K)	374.26
Noise power (dBW)	−165.09

Table 16: Uplink budget.

Elevation	$\beta = 5^\circ$	$\beta = 10^\circ$	$\beta = 15^\circ$
Received power Pr (dBW)	−132.58	−131.22	−130.14
Noise power (dBW)	−165.09	−165.09	−165.09
SNR (dB)	32.51	33.87	34.95
Margin with 20 dB (dB)	12.51	13.87	14.95

direction of the ground station is maximum, and it can be calculated as

$$\eta = \arcsin\left(\cos\beta \cdot \frac{R_E}{R_E + H}\right). \quad (17)$$

Table 17: Worst and best case for SNR in uplink.

Situation	Worst case	Best case	Difference (dB)
P_t (dBW)	16.99	16.99	0.00
G_t (dBi)	18.95	18.95	0.00
L_{FS} (dB)	157.33	136.24	21.09
L_{ATM} (dB)	0.22	0.02	0.20
L_S (dB)	0.37	0.02	0.35
L_{up} (dB)	1.00	0.00	1.00
PLF (dB)	−3.00	0.00	3.00
G_r (dBi)	−6.00	1.56	7.56
L_{SW} (dB)	0.60	0.60	0.00
P_r (dBW)	−132.58	−99.38	33.20
Noise temperature (dBK)	25.73	25.735	0.00
Noise power (dBW)	−165.09	−165.09	0.00
SNR (dB)	32.51	65.71	33.20

For different elevation angles, the value of this angle is shown in Table 19.

Pointing this antenna to the Earth increases the gain of the antenna in 4.2 dB because the gain of the antenna used has a gain more than −1.8 dBi in the directions of interest (instead of −6 dBi) [19]. The polarization can be considered always right-hand circularly polarized, so there is also a gain of 3 dB if a ground station antenna with such polarization is used.

The final result is that pointing the antenna to Nadir allows increasing the signal in 7.2 dB, which can increase the data rate in a factor of 5.

3.3. Increasing the Frequency. Using a frequency greater than 2 GHz allows using a directive antenna both in the satellite and in the ground station. Increasing the frequency has many consequences, such as the increase in the free space losses. These losses must be compensated with the gain of the antennas, but then the pointing requirement also increases. These points are going to be explained in the next section.

3.3.1. X Band. Using the X band is a good solution to increase the data rate. Although the gain of the antenna on the satellite

Table 18: Nano and microsatellite missions.

Name	Contractor	Dry mass (kg)	Band	Data rate (Mbps)
ORS-4/HawaiiSat-1 [12]	Hawaii Space Flight Laboratory (US)	55	U	0.1152
Kent Ridge 1 (KR1) [13]	NUS (Singapore)	78	X	100
LAPAN-A2 [14]	National Institute of Aeronautics and Space (Indonesia)	74	S	5
Tsubame [15]	Tokyo Institute of Technology (JP)	48.6	S	0.1
UNIFORM-1 [16]	Several Universities (JP)	49	X	10
Flock [17]	Planet Labs	5	X	200
Lemur [18]	Spire	5	S	—

Table 19: Downlink budget.

Elevation	$\beta = 5^\circ$	$\beta = 10^\circ$	$\beta = 15^\circ$
$\eta(^\circ)$	57.6	56.6	54.9

Table 20: Downlink at 8.16 GHz.

Parameter	Value
P_t (dBW)	0.58
G_t (dBi)	13.5
L_{up} (dB)	0.5
L_{FS} (dB)	173.88
L_{ATM} (dB)	0.37
PLF (dB)	0.00
G_r (dBi)	47.50
P_r (dBW)	−113.17
Noise temperature (K)	120
Bandwidth (MHz)	100
Noise power (dBW)	−127.81
SNR (dB)	14.64
Margin with 14 dB (dB)	0.64

could not be really high, the increase in free space loss can be compensated with the gain of the ground station. In Table 20, the link budget for 8.16 GHz and 100 MHz of the bandwidth is shown for an elevation angle of 15°.

These values were obtained from [20]. Noise temperature is considered without the sun. The antenna noise temperature is 2.7 K [11], but with the atmospheric attenuation [21], it increases up to 26 K. A typical equivalent temperature of a low-noise amplifier at this frequency is between 60 and 80 K [22]. With a transmission line of 0.1 dB of attenuation between the antenna and the low noise amplifier, the total noise temperature is below 120 K.

With these values of the parameters, the SNR is 14.64 dB when the antenna is pointed to the ground station and the minimum elevation is 15°, which is 0.64 dB greater than the minimum SNR required.

3.3.2. Ka Band. NASA's Jet Propulsion Laboratory has developed [23] an antenna that fits in a 1.5U of a Cubesat to be used in RainCube 6U Cubesat which is a fixed nadir-pointing satellite working at the Ka band for detecting rain with RADAR. When the antenna is deployed, it has a diameter of 0.5 m. This antenna is also going to be used [24] in NASA's Deep Space Network with a frequency of 34.2–34.7 GHz for the uplink and 31.8–32.3 GHz for the downlink. As the downlink with a Cubesat is more challenging than the uplink, we are going to show in Table 21 the link budget when using an antenna like this in a 6U Cubesat with the same orbit constraints as Xatcobeo's for elevation of 15°.

Table 21: Downlink at 32 GHz.

Parameter	Value
P_t (dBW)	6.02
G_t (dBi)	42.00
L_{FS} (dB)	192.58
L_{ATM} (dB)	6.64
L_{up} (dB)	3.00
PLF (dB)	0.00
G_r (dBi)	42.00
P_r (dBW)	−112.20
Noise temperature (K)	448
Bandwidth (MHz)	20
Noise power (dBW)	−129.08
SNR (dB)	16.88

Noise temperature is considered without the sun. The antenna noise temperature is 40 K [11], but with an attenuation of 6.64 dB [21] (0.317 dB for gas attenuation, 0.964 dB for rain attenuation, and 0.438 dB for cloud attenuation, all corrected for an elevation of 15°), the temperature at the antenna output is 236 K. A typical equivalent temperature of a low-noise amplifier at this frequency is 200 K [22]. With a transmission line of 0.1 dB of attenuation between the antenna and the low-noise amplifier, the total noise temperature is 448 K. NASA's Jet Propulsion Laboratory has designed a transponder (Iris Version 2 [25]) that can transmit 4 W. The ground station antenna is assumed to have at least the same gain as the antenna on the satellite.

With these values of the parameters, the SNR is 16.68 dB when using 20 MHz of bandwidth. This high bandwidth, combined with 26.04 minutes per day (Table 4), would allow transmitting more than 3.8 Gbyte per day.

3.4. Using Optical Communications. Wireless optical communication has several advantages compared to radio frequency communication. It requires low transmit powers and small terminal mass, while at the same time it avoids signal spectrum regulation issues and provides data rates by one order of magnitude higher than those achieved by RF communication links. Laser-based communication provides better security features that reduce the probability of interception with channel rates of several gigabits per second together in several channels (wavelength division multiplexing systems). Moreover, the downlink can be deployed by a small transmitter terminal of some centimeter aperture diameter with transmit powers below one watt and a medium-sized receiver terminal telescope of around 1-meter diameter.

Some problems that affect the link performance are the effects of atmospheric signal attenuation in addition to free-space loss, as well as the signal fluctuations induced by atmospheric index-of-refraction turbulence (IRT) or scintillation. Both effects become more severe with lower link elevation angles. Moreover, different transmission formats are required to adapt to different needs, like pointing precision, transmit power, aperture diameters, and range of link elevations. We will consider only intensity modulation and direct detection techniques in this study, as well as typical performance for penalties associated with channel degradation and pointing and tracking subsystems.

Typically in a wireless optical communication system, there are two optical subsystems in the space segment and in the ground segment: in the former, a beacon-receiver with a coarse pointing system and a data transmitter. In the ground segment, the incoming light that transmits data is collected with a telescope. After it is forwarded to a photodetector, it is also splitted into a tracking sensor, enabling a closed-loop tracking, and to a data receiver. There are also uplink beacons. Usually the communication is as follows.

(1) Acquisition. The optical satellite receiver is illuminated by the ground beacon to enable precise orientation and pointing.

(2) Tracking and Data Link. The satellite sends data, the ground station receives data and tracks the satellite using the downlink data signal as the tracking beacon.

(3) Link Termination. When the link reaches a minimum elevation angle, the link is stopped.

In this section, we will simulate the link budget of a typical wireless optical communication point-to-point data network that consists of an optical source, a transmitter, the free space channel, the optical detector, the receiver, and two pointing, acquisition, and tracking systems. We will neglect in the discussion these pointing systems and the beacons, and we will use average values for some of the penalties associated with the free space channel characteristics.

Depending on the solution adopted for LEO downlinks, we can classify the links in mono or bidirectional links. The latter uses a separate optical path for receiving and transmitting beams, while the former shares one optical channel for both. Monodirectional designs are better for calibration of the system and permits a more compact terminal. However, the wavelength selection is more difficult due to interference between the transmitter and the receiver in the tracking sensor. In the bidirectional system, we can use different transmitting and receiving wavelengths and to put them close in the spectrum allocation. Depending on the system design and link budget, a 0 dBW transmit power or more can be assumed. Sensors usually have sensitivities of −67 dBW [26] for 1.5 Gbps and a bit error rate of 10^{-6}. The possibility adopted in our simulation is a bidirectional system for the LEO satellite, with a downlink in the C-band (1530–1568 nm) and the uplink in the L-band (1600–1610 nm).

Concerning atmospheric effects, and in order to obtain a good degree of availability of the optical link, several ground stations are required and also a network optimization should be performed. The attenuation due to absorption and scattering depends on the elevation angle between the ground station and the satellite, as well as on the wavelength of the signal. Finally, the change in the atmospheric index of refraction due to turbulence causes fast and strong fluctuations of the received signal. They can be more than ±6 dB and have durations between one to several milliseconds. This effect is quantified by the power scintillation index (the normalized power variance) that has to be accounted for in the link budget calculation.

In Table 22, we have calculated link budgets for satellites with orbit heights of 400 and 900 Km and 10° and 15° elevation angles. We have considered an output power from the laser of 1 W and an aperture diameter of 4 cm at the satellite. We assume a transmission optical loss of 1.5 dB, the beam divergence of 0.04 mrad, a pointing penalty of 3 dB, and a telescope gain of 98 dB. For the communication channel, we assume a bit error rate of 10^{-6}, using the third telecom window at a wavelength of 1550 nm and an on/off key modulation format. We have also assumed a scintillation loss and atmospheric attenuation according to different elevation angles.

On the receiver side, we have a telescope with an aperture diameter of 60 cm and assumed optical losses of 6 dB. The tracking losses are 1 dB.

The signal level at the input of the receiver will be

$$P_r = P_t - L_{IM} + G_t - L_{UP} - L_{FS} - L_{ATM} - L_S - L_{track} + G_r - L_{OL}, \quad (18)$$

and the result is shown in Table 22.

The results show that the link budget oscillates between 25 and 20 dB depending on the orbit height. Moreover, it will suffer stronger differences due to atmospheric circumstances and with different transmitter or receiver situations, like telescope aperture diameters or pointing penalties.

4. Pointing Budget Analysis for Radio and Optical Communications

4.1. Sources of Error and Their Contribution to Pointing Error. A definition about pointing error source is given in the Pointing Error Engineering Handbook [27] as follows:

Table 22: Link budget for satellite with an orbit height between 400 km and 900 km.

	Parameter	$H = 400$ km		$H = 900$ km	
		10°	15°	10°	15°
Comm. system	Data rate (Gbps)	1.50	1.50	1.50	1.50
	Wavelength (nm)	1550	1550	1550	1550
	Modulation format	Intensity modulation and direct detection			
	Bit error rate	$1.0E-06$	$1.0E-06$	$1.0E-06$	$1.0E-06$
TX	Output power P_t (dBW)	0.00	0.00	0.00	0.00
	TX loss L_{IM} (dB)	1.49	1.49	1.49	1.49
	TX divergence FWHM (mrad)	0.041	0.041	0.041	0.041
	TX aperture diameter (cm)	4.00	4.00	4.00	4.00
	TX telescope gain G_t (dB)	98.18	98.18	98.18	98.18
	L_{UP} (dB)	3.01	3.01	3.01	3.01
Channel	Link distance (km)	1439	1175	2588	2224
	L_{FS} (dB)	261.34	259.58	266.44	265.12
	L_S (dB)	3.50	2.50	3.50	2.50
	L_{ATM} (dB)	4.00	3.00	4.00	3.00
RX	Aperture diameter (cm)	60.00	60.00	60.00	60.00
	RX-telescope gain G_r (dB)	121.42	121.42	121.42	121.42
	L_{track} (dB)	1.00	1.00	1.00	1.00
	Optical RX losses L_{OL} (dB)	6.02	6.02	6.02	6.02
	RX-power after losses P_r (dBW)	−60.76	−57.00	−65.86	−62.54
	Sensitivity (dBW)	−67.00	−67.00	−67.00	−67.00
	Margin with sensitivity (dB)	6.24	10.00	1.14	4.46

Table 23: Sources of pointing error.

		Spacecraft position errors:	Direction of error
ΔI	In-track	Displacement along the spacecraft's velocity vector	Parallel to ground track
ΔC	Cross-track	Displacement normal to the spacecraft's orbit plane	Perpendicular to ground track
ΔRs	Radial	Displacement toward the center of the Earth (nadir)	Toward nadir
Note: these errors are dependent of the quality of the sensors used to determine the position of the spacecraft in the orbit			
		Sensing axis orientation errors:	
$\Delta\eta$	Elevation	Error in angle from nadir to sensing axis	Toward nadir
$\Delta\phi$	Azimuth	Error in rotation of the sensing axis about nadir	Azimuthal
Note: these errors include errors in attitude determination, instrument mounting, and stability for control or pointing (e.g., jitter, thermal distortion).			
		Other errors:	
ΔT	Clock error	Uncertainty in the real observation time (if applicable)	Parallel to the Earth's equator

"Pointing error source is a phenomenon which affects pointing performance." Although this might sound as a vague definition, it is very precise, in the sense that anything that can affect the performance must be considered as error source.

The contribution of each error will lately affect either the knowledge of the orientation of a spacecraft or the knowledge of its position in the orbit. However, other intrinsic errors may affect the payload performance (e.g., a misalignment of the instrument). For the purpose of this paper, the errors are considered among these three categories.

As defined by Wertz et al. [28], the sources of pointing error can be grouped in the categories listed in Table 23.

Among the spacecraft position errors, the in-track and cross-track errors will affect the pointing independently of the elevation angle, while the radial error (i.e., the displacement in altitude) will be only considerable when the elevation angle is different than 90 degrees. Moreover, for orientation errors, the error in azimuth (i.e., the rotation about the axis toward nadir) will only affect the pointing for elevations different than 90 degrees too. Further, the clock error may not

Table 24: Achievable accuracy of different technologies used for attitude determination.

Type of sensor	Attitude measurement accuracy
Magnetometer	$30'$ (0.5°)
Earth sensor	$6'$ (0.1°)
Fine sun sensor	$1'$ (0.01667°)
Star sensor	$1''$ (0.00028°)

Table 25: List of a selection of available sensors for Cubesat with their respective measurement accuracy.

Sensor brand and model	Attitude measurement accuracy
STELLA [30]	$2.4'$ (0.04°)
Sinclair ST-16 [31]	$7''$ (0.002°)
NST-1 Star sensor [31]	$7''$ (0.002°)
MAI-SS Space Sextant [31]	$41''$ (0.013°)

affect a communication device if it is transmitting within a window waiting for the link to close, but may be critical if the transmission is automatically started right in the moment that the spacecraft believes it is in the field of view of the ground station.

Furthermore, among all sources of pointing errors listed in Table 23, the one that has the most direct impact to the pointing accuracy is the error in the angle from nadir to the sensing axis, $\Delta\eta$, which also will impact the magnitude of the error in rotation of the sensing axis about nadir, $\Delta\phi$.

4.2. Different Pointing Requirements Depending on the Beamwidth. Ultimately, the requirements that will drive the design of the Attitude Determination and Control subsystem are

(i) The pointing accuracy

(ii) The pointing stability (e.g., due to the jitter that is out of the limits of the actuators)

(iii) The orbital knowledge

The narrower the field of view of the instrument, the more precise the pointing requirements.

For attitude determination, according to [29], the accuracy that can be obtained using different technologies is depicted in Table 24.

However, because sensor misalignments and actuator errors will detriment the total accuracy, these values cannot be treated as final error. Also, these are values achievables on full-size spacecrafts, while Cubesat sensors are way out of that range, as depicted with the selection of available hardware specifically designed for Cubesats in Table 25.

The less restrictive case is for UHF-band communications with dipole antennas, where the radiation pattern of the antenna is theoretically omnidirectional. However, when looking for more data throughput, the frequency of the communication channel increases rapidly while the wavelength decreases, and so does the beamwidth. The latest ultimately will also be impacted by the transmission antenna diameter, where bigger values will increase the gain but will make the beamwidth decrease, making requirements more restrictive for pointing accuracy. This is a system trade-off that will have to be made for all particular missions.

Table 26: X band antenna losses vs pointing accuracy.

Angle deviation	Losses (dB)
21°	3.0
12°	1.0
4°	0.1

Table 27: Ka band antenna losses vs pointing accuracy.

Angle deviation	Losses (dB)
0.58°	3.0
0.32°	1.0
0.10°	0.1

In particular, for the case of optical communications presented in this work, a divergence half-power beamwidth of 0.041 mrad is the driving requirement. When calculating the pointing error, the root sum square of the values presented in Table 23 must be below the value of the divergence half-power beamwidth.

4.3. Analysis Applied to the X Band Radio Link. The antenna described in [20] has a directivity of 13.5 dBi, so the satellite does not need a fine pointing in order to have low pointing losses. Table 26 shows the losses as a function of pointing precision.

Active AOCS subsystems providing enough pointing accuracy for using the X band in the radio link are currently available. For example, a commercial mission based on Cubesats [17] is providing a 200 Mbit downlink channel in this band.

4.4. Analysis Applied to the Ka Band Radio Link. The antenna described in [23] is very directive, so the satellite needs a fine pointing in order to have low pointing losses. Table 27 shows the losses as a function of pointing precision.

Even though there are no current missions based on Cubesat using Ka and Ku bands, the available commercial AOCS subsystems (Tables 24 and 25) provide enough pointing accuracy for these bands.

4.5. Analysis Applied to an Optical Communication Using a Ground Beacon. For the purpose of this analysis, two reference orbits, one of 400 km and the other of 900 km, were considered. As mentioned before, the resulting root sum square must be kept below the divergence. As suggested by [28], a good way to start budgeting the pointing is assigning the same accuracy requirement for each relevant source of error. In the case of optical communications, the clock error can be diminished taking actions to prevent a negative impact. In

Table 28: Pointing error budgets for optical communications at 400 kilometers.

PES	Error in source	Pointing error (mrad)				
		$\beta = 15^\circ$	$\beta = 20^\circ$	$\beta = 45^\circ$	$\beta = 60^\circ$	$\beta = 90^\circ$
Attitude errors:						
Azimuth	0.002°	0.0317	0.0309	0.0232	0.0164	0.0000
Nadir angle	0.002°	0.0349	0.0349	0.0349	0.0349	0.0349
Position errors:						
In-track	2 meters	0.0007	0.0009	0.0027	0.0039	0.0050
Cross-track	2 meters	0.0017	0.0020	0.0036	0.0044	0.0050
Radial	2 meters	0.0015	0.0018	0.0024	0.0021	0.0000
Root sum square		*0.0472*	*0.0467*	*0.0422*	0.0391	0.0356

Table 29: Pointing error budgets for optical communications at 900 kilometers.

PES	Error in source	Pointing error (mrad)				
		$\beta = 15^\circ$	$\beta = 20^\circ$	$\beta = 45^\circ$	$\beta = 60^\circ$	$\beta = 90^\circ$
Attitude errors:						
Azimuth	0.002°	0.0295	0.0287	0.0216	0.0153	0.0000
Nadir angle	0.002°	0.0349	0.0349	0.0349	0.0349	0.0349
Position errors:						
In-track	2 meters	0.0005	0.0006	0.0013	0.0018	0.0022
Cross-track	2 meters	0.0009	0.0010	0.0017	0.0020	0.0022
Radial	2 meters	0.0008	0.0008	0.0010	0.0009	0.0000
Root sum square		*0.0458*	*0.0452*	*0.0411*	0.0382	0.0350

such case, the initial requirement will be the total accuracy divided by the square root of 5:

$$\text{Initial accuracy} = \frac{0.041}{\sqrt{5}}\,\text{mrad} = 0.001051^\circ. \quad (19)$$

Cubesats can use optic communications using two pointing devices as in [32]. The first one requires pointing the satellite with subdegree level to the ground station using a GPS to track the position and velocity. Then, a beacon from the ground station is used to point precisely using a modified star tracker. As an example, [33] presents a device with ±2.5 mrad of angular range (±0.14°) and 0.05 μrad of resolution.

Current AOCS subsystems (Tables 24 and 25) provide enough accuracy for the first stage of the pointing subsystem. This initial stage is complemented by using adaptable internal mirrors as a second stage. This two-stage pointing system is capable of providing the required accuracy of 0.041 mrad = 0.0023°.

4.6. Analysis Applied to an Optical Communication without Using a Ground Beacon. With respect to orbit determination accuracy, as concluded with the developed made by Joplin et al. [34], a precision of 2 meters can be achieved using a dual-frequency GPS receiver. Now, considering the best case, with perfect alignment of the available star sensor, the use of a very precise dual-frequency GPS, and considering no time synchronization errors, the resulting pointing error budget will be the one presented in Tables 28 and 29 for the altitudes considered in this analysis. Moreover, Figures 4 and 5 show the contribution of each source of error to the total error with respect to the elevation angle as seen from the ground.

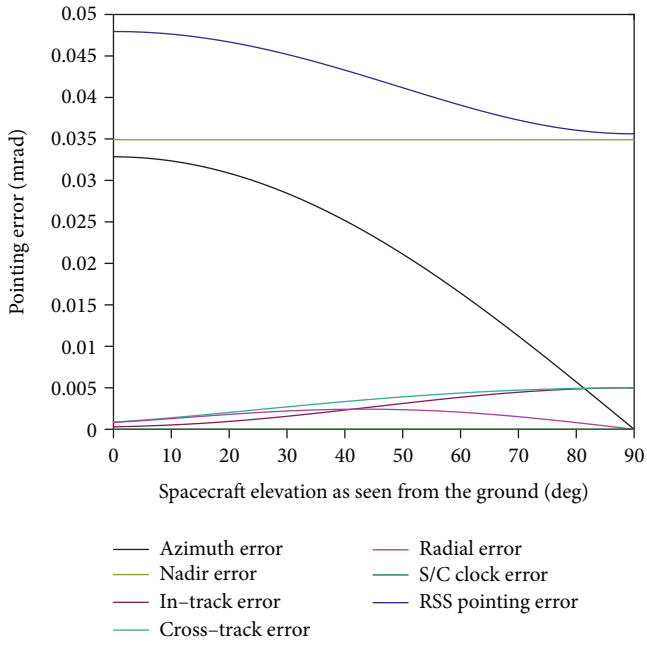

Figure 4: Pointing error as function of the elevation angle for a Spacecraft located at 400 kilometers.

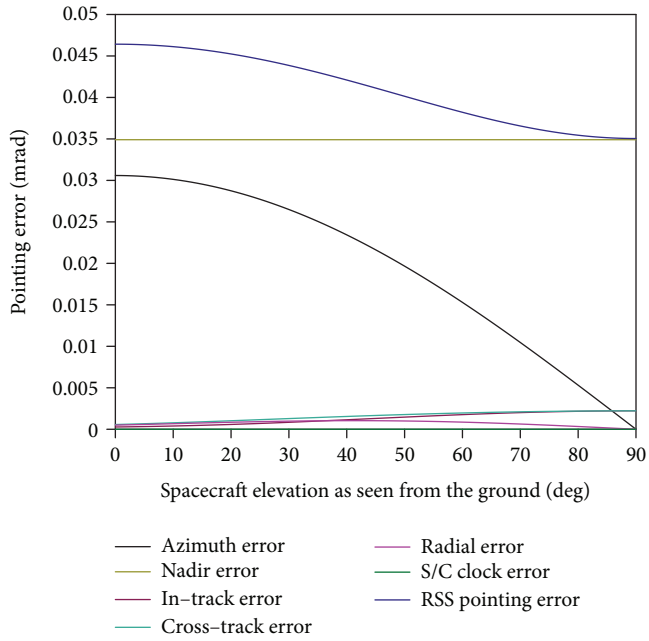

Figure 5: Pointing error as function of the elevation angle for a Spacecraft located at 900 kilometers.

Table 30: Pointing error budgets for optical communications at 400 kilometers with lower attitude error.

PES	Error in source	Pointing error (mrad)				
		$\beta = 15^\circ$	$\beta = 20^\circ$	$\beta = 45^\circ$	$\beta = 60^\circ$	$\beta = 90^\circ$
Attitude errors:						
Azimuth	0.001°	0.0159	0.0154	0.0116	0.0082	0.0000
Nadir angle	0.002°	0.0349	0.0349	0.0349	0.0349	0.0349
Position errors:						
In-track	2 meters	0.0007	0.0009	0.0027	0.0039	0.0050
Cross-track	2 meters	0.0017	0.0020	0.0036	0.0044	0.0050
Radial	2 meters	0.0015	0.0018	0.0024	0.0021	0.0000
Root sum square		0.0384	0.0383	0.0371	0.0364	0.0356

Table 31: Pointing error budgets for optical communications at 900 kilometers with lower attitude error.

PES	Error in source	Pointing error (mrad)				
		$\beta = 15^\circ$	$\beta = 20^\circ$	$\beta = 45^\circ$	$\beta = 60^\circ$	$\beta = 90^\circ$
Attitude errors:						
Azimuth	0.001°	0.0148	0.0144	0.0108	0.0076	0.0000
Nadir angle	0.002°	0.0349	0.0349	0.0349	0.0349	0.0349
Position errors:						
In-track	2 meters	0.0005	0.0006	0.0013	0.0018	0.0022
Cross-track	2 meters	0.0009	0.0010	0.0017	0.0020	0.0022
Radial	2 meters	0.0008	0.0008	0.0010	0.0009	0.0000
Root sum square		0.0379	0.0378	0.0366	0.0358	0.0350

These results show that this will not be feasible for elevations of 45 degrees or lower and thus a better performance in the sources of error will be required.

Now, assuming an increase in performance on the attitude determination about the azimuth to 0.001 degrees, the results are more prominent, as can be seen in Tables 30 and 31.

Results presented in Tables 30 and 31 show that available commercial AOCS subsystems for Cubesats (Tables 24 and 25) do not provide enough accuracy and stability for

implementing optical communications links without a two-stage pointing scheme.

5. Conclusions

In this paper, a complete analysis of different alternatives of communication subsystems for Cubesats missions is presented. For low-demanding communication missions, such as educational university projects, the use of the UHF band transceivers with quasi-onmidirectional antennas and no pointing system provides enough link capacity using a low complex Cubesat platform. As an example of this kind of mission, a detailed study of the Xatcobeo communication subsystem is presented. On the other hand, scientific and commercial applications demand an increasing communication capacity that requires the use of higher frequencies to use a wider bandwidth as well as higher antenna gains, both at the spacecraft and at the Ground Station. The use of these bands require, for a precise pointing of the Cubesat antenna, the use of active AOCS subsystems, which are currently commercially available.

Finally, a feasibility analysis of an optical communication subsystem for Cubesats is presented. This analysis shows that this solution is technically viable, but it requires a two-stage pointing system, since the available AOCS subsystems do not provide enough accuracy and stability for the pointing requirements.

In conclusion, the authors have presented in this paper a rigorous calculation in different frequency bands (UHF, X and Ka bands, and optical communications) of the signal-to-noise ratio and the pointing accuracy that is needed to achieve the maximum transmission speed at each frequency band from the satellite to the ground station, and therefore the requirements that the AOCS must have, as well as the limitations of current systems, specially in optical communications.

Data Availability

The data used to support the findings of this study are included within the article.

Conflicts of Interest

The authors declare that there is no conflict of interest regarding the publication of this paper.

Acknowledgments

The work of F. Aguado is supported by the Spanish Ministry of Economy, Industry and Competitiveness under project IMONss (ESP2016-79184-R) and the Interreg Sudoe programme under grant number SOE1/P4/E0437 (FireRS project). The work of A. Villa is supported by the Galician Center for Innovation in Aerospace Technology (CINAE). The work of M. Arias is partially supported by the Spanish National Research and Development Project (TEC2015-65353-R), by the European Regional Development Fund (ERDF), and by Galician Regional Government under project GRC2015/018 and under agreement for funding AtlantTIC (Atlantic Research Center for Information and Communication Technologies).

References

[1] A. Castro, R. Walker, F. Emma, F. Aguado, R. Tubío, and W. Balogh, "Hands-on experience: the HumSAT system and the ESA GEOID initiative," *ESA Bulletin*, vol. 149, pp. 45–50, 2012.

[2] P. Faure, A. Tanaka, and M. Cho, "Toward lean satellites reliability improvement using HORYU-IV project as case study," *Acta Astronautica*, vol. 133, pp. 33–49, 2017.

[3] A. Mehrparvar, *CubeSats Design Specifications (Rev. 13)*, California Polytechnic State University, 2014.

[4] F. Aguado-Agelet, C. Martínez, O. Rubiños-López, M. Arias, and E. Sarmiento, "Xatcobeo: educational CubeSat project selected by the European Space Agency (ESA) for the maiden flight of Vega," in *Internacional Conference of Education, Research and Innovation (ICERI'08)*, pp. 1–4, Madrid, Spain, 2008.

[5] *Xatcobeo Project. Reference LEX-EP/2008/RW/24*, European Space Agency, 2008.

[6] https://www.agi.com/products/engineering-tools.

[7] A. J. Vázquez-Alvarez, R. Tubío-Pardavila, A. González-Muiño, F. Aguado-Agelet, M. Arias-Acuña, and J. A. Vilán-Vilán, "Design of a polarization diversity system for ground stations of CubeSat space systems," *IEEE Antennas and Wireless Propagation Letters*, vol. 11, pp. 917–920, 2012.

[8] ITU-R, *P.618-9: Propagation Data and Prediction Methods Required for the Design of Earth-Space Telecommunication Systems*, International Telecommunication Union, 2017.

[9] ITU-R, *P.676-10: Attenuation by Atmospheric Gases*, International Telecommunication Union, 2016.

[10] K. S. Ygnvesson, J. F. Johansson, Y. Rahmat-Samii, and Y. S. Kim, "Realizable feed-element patterns and optimum aperture efficiency in multibeam antenna systems," *IEEE Transactions on Antennas and Propagation*, vol. 36, no. 11, pp. 1637–1641, 1988.

[11] ITU-R, *P.372-8: Radio Noise*, International Telecommunication Union, 2016.

[12] eoPortal, "eoPortal.org - ORS-4-HiakaSat," https://directory.eoportal.org/web/eoportal/satellite-missions/pag-filter/-/article/ors-4-hiakasat.

[13] eoPortal, "eoPortal.org - Kent-Ridge-1," https://directory.eoportal.org/web/eoportal/satellite-missions/pag-filter/-/article/kent-ridge-1.

[14] eoPortal, "eoPortal.org - LAPAN-A2," https://directory.eoportal.org/web/eoportal/satellite-missions/l/lapan-a2.

[15] eoPortal, "eoPortal.org - Tsubame," https://directory.eoportal.org/web/eoportal/satellite-missions/pag-filter/-/article/tsubame.

[16] eoPortal, "eoPortal.org - UNIFORM-1," https://directory.eoportal.org/web/eoportal/satellite-missions/pag-filter/-/article/uniform-1.

[17] eoPortal, "eoPortal.org - Flock," https://directory.eoportal.org/web/eoportal/satellite-missions/f/flock-1.

[18] eoPortal, "eoPortal.org - Lemur," https://directory.eoportal.org/web/eoportal/satellite-missions/l/lemur.

[19] V. Ruiz, R. Tubío, D. Hermida, and F. Aguado, "Antennas RF design," Xatcobeo Technical Note XAT-51600-TNO-003-UVIGO.INTA, University of Vigo, 2011.

[20] T. Fukami, H. Watanabe, H. Saito et al., "Field tests of 348 Mbps high speed downlink system for 50-kg class satellite," in *30th International Symposium on Space Technology and Science (ISTS)*, Hyogo, Japan, June 2015.

[21] D. D. Morabito, "A comparison of estimates of atmospheric effects on signal propagation using ITU models: initial study results," IPN Progress report 42-199, SAO/NASA Astrophysics Data System, 2014, https://ipnpr.jpl.nasa.gov/progress_report/42-199/199D.pdf.

[22] J. Schleeh, N. Wadefalk, P. A. Nilsson, J. P. Starski, and J. Grahn, "Cryogenic broadband ultra-low-noise MMIC LNAs for radio astronomy applications," *IEEE Transactions on Microwave Theory and Techniques*, vol. 61, no. 2, pp. 871–877, 2013.

[23] N. Chahat, R. E. Hodges, J. Sauder, M. Thomson, E. Peral, and Y. Rahmat-Samii, "Cubesat deployable Ka-Band mesh reflector antenna development for earth science missions," *IEEE Transactions on Antennas and Propagation*, vol. 64, no. 6, pp. 2083–2093, 2016.

[24] N. Chahat, R. E. Hodges, J. Sauder, M. Thomson, and Y. Rahmat-Samii, "The deep-space network telecommunication CubeSat antenna: using the deployable Ka-band mesh reflector antenna," *IEEE Antennas and Propagation Magazine*, vol. 59, no. 2, pp. 31–38, 2017.

[25] Jet Propulsion Laboratory, "Iris V2 CubeSat deep-space transponder (IRIS)," https://www.jpl.nasa.gov/cubesat/missions/iris.php.

[26] https://www.kyosemi.co.jp/en/communication/ingaas_apd-tia_receiver/kpdxa2gk/.

[27] *ESA Pointing Error Engineering Handbook, ESSB-HB-E-003 Issue 1 Revision 0*, European Space Agency, 2011.

[28] J. R. Wertz, D. F. Everett, and J. J. Puschell, *Space Mission Engineering: The New SMAD (SME-SMAD)*, Microcosm Press, 2011.

[29] G. Zhang, *Star Identification: Methods, Techniques and Algorithms*, Springer, 2017.

[30] http://www8.informatik.uni-wuerzburg.de/en/wissenschaftforschung/stella/.

[31] http://www.cubesatshop.com.

[32] D. K. L. Oi, A. Ling, G. Vallone et al., "CubeSat quantum communications mission," *EPJ Quantum Technology*, vol. 4, no. 1, p. 6, 2017.

[33] Z. Hu, Z. Song, S. Tong, Z. Xin, H. Song, and H. Jiang, "Modeling of fine tracking sensor for free space laser communication systems," in *2009 Symposium on Photonics and Optoelectronics*, pp. 1–4, Wuhan, China, 2009.

[34] A. J. Joplin, E. G. Lightsey, and T. E. Humphreys, "Development and testing of a miniaturized, dual-frequency software-defined GPS receiver for space applications," in *Proceedings of the 2012 International Technical Meeting of the Institute of Navigation*, pp. 1468–1525, Newport Beach, CA, USA, January 2012.